Master's thesis

Master's Programme in Atmospheric Sciences

Meteorology

Utilisation of drones in wind measurements: an analysis of wind data gathered with a drone-bound ultrasonic anemometer

Kalle-Matti Koivula

March 25, 2023

Supervisor(s):

M.Sc. (Eng) Klaus Haikarainen

M.Sc. (Met) Jarkko Hirvonen

Senior University Lecturer Jouni Räisänen

Examiner(s): Heikki Järvinen

Jouni Räisänen

University of Helsinki

Faculty of Science

PL 64 (Gustaf Hällströmin katu 2a)

00014 Helsingin yliopisto

HELSINGIN YLIOPISTO — HELSINGFORS UNIVERSITET — UNIVERSITY OF HELSINKI

Tiedekunta — Fakultet — Faculty	Koulutusohjelma — Utbildningsprogram — Degree programme
Faculty of Science	Master's Programme in Atmospheric Sciences Meteorology

Tekijä — Författare — Author

Kalle-Matti Koivula

Työn nimi — Arbetets titel — Title

Utilisation of drones in wind measurements: an analysis of wind data gathered with a drone-bound ultrasonic anemometer

Työn laji — Arbetets art — Level	Aika — Datum — Month and year	Sivumäärä — Sidantal — Number of pages
Master's thesis	March 25, 2023	52

Tiivistelmä — Referat — Abstract

In this thesis we try to find the measurement accuracy of our dronebound wind measurement setup and if the quality of the measurements is high enough for operational usage. The thesis goes over the most important theoretical concepts concerning effects of wind in the boundary layer.

In the thesis we analyze wind data gathered by a drone-bound anemometer, and introduce a direct method of measuring wind with a UAV. The data includes stationary wind data gathered at height of 30 metres, as well as vertical wind profiles to 500 metres above ground level. The data is compared to reference data from a 30 metre wind mast and automatic radiosoundings. The measurements were conducted in Jokioinen, Finland between the 2nd of September 2022 and 10th of October 2022. Total of 20 measurement flights were conducted, consisting of 14 stationary wind measurements and six wind profile measurements.

We found out the stationary wind measurement quality to be comparable with earlier studies. The vertical wind profile measurements were found to be hard to analyze, as the reference measurement was not as compatible as we had hoped for. The difference between automatic radiosoundings and our profile measurements was distinctly greater than the difference between the stationary drone and wind mast measurements.

Lastly some optimization and improvements to the measurement arrangement are discussed. The application of these improvements and modifications will be left as future endeavour for some willing individual.

Avainsanat — Nyckelord — Keywords

Drone, Unmanned aerial vehicle, Wind measurement, Boundary layer, Data analysis

Säilytyspaikka — Förvaringsställe — Where deposited

Kumpula Campus Library, Gustaf Hällströmin katu 2, 00560, Helsinki

Muita tietoja — Övriga uppgifter — Additional information

Contents

List of Symbols

κ	Von Kármán constant	0.41
ψ	Stability parameter	
ρ	Density (of air)	kg/m^3
d	Zero plane displacement	m/s
e	Water vapour pressure	Pa
f	Coriolis parameter	$1/s$
M	Molecular mass of air	28.96 g/mol
p	Pressure	Pa
R	Universal gas constant (air)	287.05 J/kgK
T	Temperature	K
U	Zonal component of wind	m/s
u_*	Friction velocity	m/s
u_z	Log wind profile	m/s
V	Meridional component of wind	m/s
V_g	Geostrophic wind	m/s
z	height	m
z_0	Roughness length	m

1. Introduction

An unmanned aerial vehicle (UAV), or drone, is defined as a crewless aircraft that is controlled remotely. Like many other inventions, drones are also of military origin, as they were originally designed for military missions deemed too dangerous for military personnel to conduct [Kozera, 2018].

As the drone controlling technology improved and the cost of the different UAVs decreased, the usage of drones has widened; movie industry uses drones for precise aerial filming, in bigger cities products are being delivered by drones and even drone racing has become a sport and a hobby for many. But most importantly, drones have been realized to have numerous applications in science [Pinto et al., 2021], for example atmospheric profiling and study of atmospheric fluxes.

The usage of drones in atmospheric profiling has a lot of promise, as a great in situ observational gap exists in the surface layer, atmospheric boundary layer, and lower free troposphere, because there has this far been no feasible way to probe the lower atmosphere with a sufficient time resolution. This leads us to a situation where our data does not have the temporal or spatial requirements for high-accuracy short-term model predictions of impactful weather. Even though we can probe the atmosphere with automatic radiosonde measurements, the frequency of these measurements is simply not enough. Usage of drones could help us with this dilemma [Pinto et al., 2021].

In this thesis we will be discussing the usage of drones in wind measurements. Specifically, wind data gathered with a dronebound anomemeter will be compared with data gathered by a traditional wind mast. The aim of this is to find out how our measurement arrangement compares to previous studies and existing measurement standards. We are also trying to find out if the quality of our measurement arrangement is high enough for operational usage. Possible improvements to the measurement arrangement will be considered.

In the following sections we will first be going through the necessary theoretical concepts in section 2, then the details about our measurements and measurement arrangement as well as data structure in section 3. The results of our data analysis for vertical wind profiles and stationary wind measurements will follow in section 4, and lastly we present our concluding remarks as well as proposed improvements to our measurement arrangement in section 5.

2. Theoretical background

2.1 Wind in the Boundary Layer

In the following subsections we are going to go through the most important concepts that govern the flow of air in the lower parts of the atmosphere. We will first go through the basics of how geostrophic wind governs the flow in the free atmosphere. After this we will be discussing how turbulent drag slows down the wind in the surface layer and how that can in certain situations lead to a logarithmic wind profile. Lastly we will be shortly discussing the effect of turbulence on the dronebound wind measurements.

2.1.1 Geostrophic wind

From the scale analysis of the horizontal momentum equations, we know that in mid-latitudes in the free atmosphere, the Coriolis-force and pressure gradient force are approximately in balance. This gives us the geostrophic approximation in scalar form [Holton, 2013]:

$$-fv \approx -\frac{1}{\rho}\frac{\partial p}{\partial x}; \quad fu \approx -\frac{1}{\rho}\frac{\partial p}{\partial y} \tag{2.1}$$

where $f \equiv 2\Omega sin(\phi)$ is the Coriolis parameter. From this relationship we can define a horizontal velocity field, that is identical to the identity 2.1 [Holton, 2013]:

$$\vec{V_g} \equiv \hat{k} \times \frac{1}{\rho f}\nabla p \tag{2.2}$$

This velocity field is called *geostrophic wind*. This simply means, that the pressure distribution determines the geostrophic wind field.

The definition of geostrophic wind is handy, as in the midlatitudes it can be used as sufficiently good approximation for the mean horizontal wind field. Notably, the geostrophic wind does not contain a time tendency term, thus it can not be used for prediction of the evolution of the wind field [Holton, 2013].

2.1.2 Logarithmic wind profile

As in this thesis we are focusing on wind measurements in the planetary boundary layer (PBL), it is important to understand the logarithmic wind profile (figure 2.1). Log wind profile tells us, that in the surface layer (roughly the first 100 meters of PBL), when the atmosphere is neutrally stratified, the mean wind increases linearly with the logarithm of height.

The shape of the wind profile (figure 2.1) is caused by frictional drag causing the wind speed to decrease near the ground and pressure gradient force drives the increase in wind speed with height [Emeis and Turk, 2007].

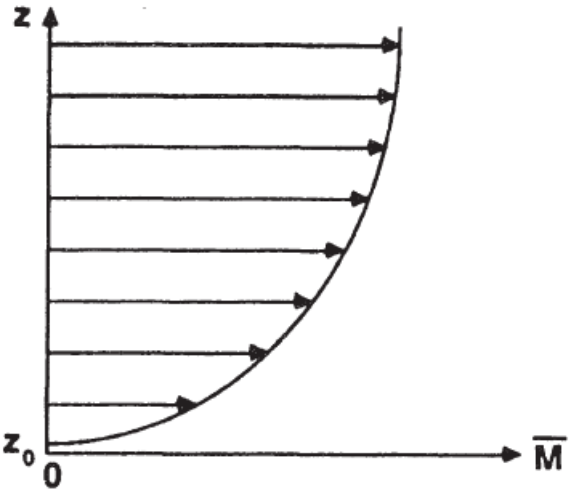

Figure 2.1: Logarithmic variation of mean wind speed with height in neutrally stratified surface layer [Stull, 1988].

Log wind profile can be mathematically defined as:

$$u_z = \frac{u_*}{\kappa}\left[\ln\frac{z-d}{z_0} + \psi(z, z_0, L)\right] \tag{2.3}$$

where u_* is the friction velocity ($\frac{m}{s}$), κ is the Von Kármán constant (0.41), d is the zero plane displacement (in metres), ψ is a stability term where L is the Obukhov length from Monin-Obukhov similarity theory and z_0 is the roughness length (in meters).

Roughness length is a parameter used in vertical wind speed equations that estimate horizontal wind speeds near the ground level. In log wind profile, roughness length

tells us the height at which wind speed becomes zero, if no obstacles that would slow the wind are present. Roughness length is important when analysis of the aerodynamical properties of the surface is deemed necessary [Stull, 1988].

The name roughness length comes from the fact that it is highly dependent on the height of the roughness elements of the terrain; i.e. smoother surfaces like sea surface have smaller roughness length than rougher surfaces such as urban areas like city centres [Stull, 1988].

In neutrally stratified boundary layer, this reduces to:

$$u_z = \frac{u_*}{\kappa}\left[\ln\frac{z-d}{z_0}\right] \tag{2.4}$$

2.1.3 Effect of turbulence on drone measurements

Turbulence is an important concept when it comes to measurement of wind and especially aircraft safety. In layman's terms [Britannica, 2023], turbulence is defined as small scale, irregular air motions, that vary in speed and direction. In the surface layer, turbulence varies diurnally. This occurs, because the heating of surface air by solar radiation creates updrafts. Combined with the effect of natural and man-made roughness elements, turbulence can make the winds near the ground level extremely irregular.

Turbulence complicates the drone measurements. First of all, even though we have temporally dense data, averaging of the data must be conducted. This is mainly because of turbulence and the fact that our reference measurement and dronebound measurements are not measured in exactly the same location, but about 20 meters apart, therefore individual data points can differ quite a lot. Thus averaging is conducted.

Secondly, the eddies can and will affect the drone in flight. This can be potentially dangerous, as the drone used in the measurements is large and heavy. The possibility of aircraft failure is the highest when conducting vertical wind profiles, as mean wind speed increases with height. Another effect caused by turbulence is the "rocking" of the drone; when airflow is clearly turbulent, the drone tends to change it's roll and pitch angles quite rapidly. This can cause errors in the measurements.

2.2 Working principle of ultrasonic anemometers

The working principle of ultrasonic anemometers, often also called sonic anemometers, is based on the wind dependence of the speed of sound. The main advantage in using a ultrasonic anemometer is its linearity and short response time; usually the magnitude of milliseconds, thus being optimal for measuring highly fluctuating wind. In combination with the aforementioned features, ultrasonic anemometers are also easy to use. Because of these properties, ultrasonic anemometers have proved their usefulness in the study of planetary boundary layer.

When a sound wave propagates in a medium, its velocity depends on the elastic properties of the medium. In our case, the medium is air. Thus, when the sound wave propagates in the air, its transmission speed is the sum of the velocity of the medium and the velocity of sound respect to the medium.

The sonic anemometer used in this study (Anemoment TriSonica Mini Wind and Weather Sensor) has the same operating principle as other similar ultrasonic anemometers; it consists of two pairs of piezoelectric transducers, that are used to both transmit and receive. The pulses move in opposite directions in the same path for each axis of measurement between the transducers. The anemometer then measures the difference between the propagation speed of the pulses sent in the opposite directions. This value represents the average airflow that has crossed a cylinder, the size of which depends on the path length and the diameter of the transducer.

Generally ultrasonic anemometers have been divided into two classes depending on the way of transmitting the sound waves; the first class is the one TriSonica Mini belongs in: pulse anemometers. In nutshell, pulse anemometer's transducers send sonic pulses along the axis of interest. Pulses moving with the wind arrive earlier than pulses moving against the wind. By simple differencing of the sound speeds in the two opposite directions, the wind component along the axis of measurement can be calculated.

The second class is the continuos-phase sonic anemometers. Continuous-phase sonic anemometers, like their name hints, transmit a continuous beam of sonic energy between the transducers. The phase of the received signal is then compared to a reference phase. Through finding the difference between the reference phase and the measured phase, wind speed and direction can be calculated.

The operating principle of the measurement is based on the fact, that when a sound

wave propagates through air, a time lag gets produced, which is dependent on the velocity and the direction of the wind.

There are a few equations which govern the operating principle of ultrasonic anemometry. First of them is the equation for the speed of sound in still, dry air:

$$C = \sqrt{\frac{\gamma RT}{M}} \tag{2.5}$$

in which γ is the ratio of specific heats at constant pressure and volume, R is the universal gas constant and M is the molecular mass of the gas in question, which in our case is air.

One could think that the wind speed could be found by simply measuring the speeds of two sound pulses moving in different directions, and then averaging the pulses' speed difference. Anemometers that rely on this measuring principle exist, but may yield erroneous results in certain situations, i.e when measuring extremely strong or weak winds. Thus more sophisticated algorithms, that acknowledge the dependency of speed of sound on temperature and humidity, are needed. This is why the instruments often include precise thermometers to calculate the sonic velocity on the fly.

However, if air has a high amount of water vapor in it, i.e. the air is humid, the sonic speed might increase and thus cause unwanted errors in the wind speed calculations. This can be accounted for by using an empirical equation for speed of sound in humid air [Camuffo, 2019]:

$$C = 2006.7\sqrt{T(1 + 0.3192\frac{e}{p})} \text{ (cm } s^{-1}) \tag{2.6}$$

In which e is the water vapour pressure, p is the atmospheric pressure and T is the temperature.

After finding the speed of sound by using equations 2.5 or 2.6, the anemometer then calculates the wind speed and angle in reference to the transducer alignment by first calculating the difference in the sonic transit time in the two opposite directions:

$$\Delta t = \frac{2Lucos(\theta)}{C^2(1 - \frac{(ucos(\theta))^2}{C^2})} \tag{2.7}$$

In which L is the distance between the transducers, $ucos(\theta)$ is the speed component along the axis of measurement (Figure 2.2), C is the speed of sound in the medium and Δt is the difference in the sonic transit time in the two opposite directions.

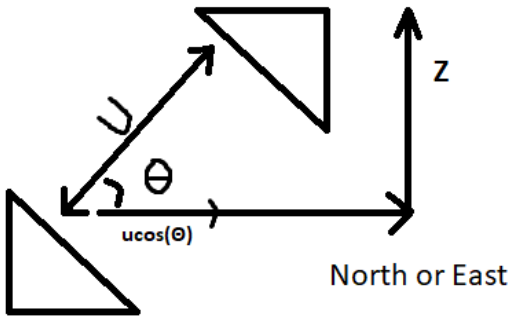

Figure 2.2: A schematic on the measuring geometry. Transducer pairs are oriented towards cardinal directions, thus $ucos(\theta)$ gives us either the zonal or the meridional component of the wind.

Equation 2.5 is known as the basic equation for ultrasonic anemometry, and the anemometer uses it as a proxy to measure the speed component $ucos(\theta)$ [Camuffo, 2019].

2.3 Unmanned Aerial Vehicles (UAVs)

At the time of writing this thesis, two types of UAVs are used in measurements of wind speed and direction: fixed-wing (FW) and rotary-wing (RW) configurations. In this thesis, we will be mostly focusing on the latter, as our measurements were conducted with a rotary-wing configuration.

The usage of rotary-wing UAVs has become more common in the scientific community as of late. After the realization that RW UAVs work as excellent chassis for different types of measurement devices, as well as bringing the possibility of almost unlimited flexibility in flight patterns to the table, the usage of UAVs, has rapidly gained increased popularity especially in atmospheric research [Wetz et al., 2021].

The most important features of using RW UAVs in atmospheric research include the aforementioned spatial flexibility, that had been unheard-of before the early 2010s, as well as the relative inexpensivity of the aircraft. These features combined with the flexibility in usage, i.e. the possibility of adding and removing payload from the UAV, and the ability to stay stationary in the air, give us a measurement device that is highly versatile, and is only really limited in use by the weight of the payload and certain weather events, such as heavy rain [Wetz et al., 2021].

When it comes to the measurement of wind with UAVs, two main ways of measurement have been described in literature. First of these, and the one we ended up using in our measurements, is to use a RW UAV as a measurement chassis, and attach an ultrasonic anemometer, or another comparable measurement device, to the drone.

The first measurement concept has been relatively popular, but not as popular as the second measurement concept: approximating the wind measurement from the onboard sensors of the avionic systems of the UAV. This basically means, that we can find the direction and the speed of wind by studying the orientation angles that the inertial measurement unit (IMU) of the drone measures and uses for staying stable in the air [Wetz et al., 2021].

RW UAV wind measurements are not without faults, however; there are a few important factors, that should be taken into account when possible. First of these is the effect of propeller downwash, i.e. the vertical flow that is induced into the wind flow by the propellers of the UAV. This added flow component can cause errors to the measurement, and thus should be taken into account in one way or another. This can be done by creating a correction function that depends on the aerodynamical properties of the measurement arrangement ([Neumann et al., 2012]) or by trying to minimize the effect of downwash by optimizing the sensor location ([Wilson et al., 2022]). In this thesis' case, the latter was conducted.

Another limiting factor of the UAV measurement system is the weight of the payload. Higher payloads reduce battery lifetime, which means shorter continuous measurement periods. This can be compensated for with extra battery sets. This is hardly a problem in our measurement setup, as the sonic anemometer used was very light, measuring at only 50 grams of weight. Payloads this small barely affect the lifetime of batteries.

The third limiting factor is weather. As UAVs are considered aircraft, aviation security must be taken into account. This basically means, that flying in certain weather conditions is advised against and might cause dangerous situations. These include strong wind events, strong wind shear, and freezing conditions in which the propellers and motors might start to gather ice. This means that UAVs are not well suited for wintery conditions. This can also cause major problems when atmospheric conditions are not properly known. Thus the UAV should have adequate safety features.

The fourth and last limiting factor is the aviation law. At the moment the piloting of UAVs is strictly regulated by aviation laws, as they have been used to interfere with air traffic in the past. Because of these incidents and overall will to make aviation as safe as possible, strict rules have been applied to piloting drones. These include, for instance, a maximum flying height, distance-keeping from people and buildings and categorization of UAVs based on their features such as size, speed and inclusion of cameras. Even though exceptions for the regulations can be made when deemed necessary by the government department in control of these regulations (in Finland's case Traficom), this adds a layer of bureaucracy to the mix, which is often seen as negative.

2.4 Mathematical and statistical methods

In the following sections, the most important mathematical and statistical methods used in the data analysis for this thesis will be introduced.

2.4.1 Vector calculus

Wind is a vector quantity. This vector form can be either two- or three-dimensional depending on the application at hand. For example meteorological surface observations often measure two-dimensional wind speed, whereas researchers studying atmospheric fluxes might be more interested in the complete three-dimensional form.

For the analysis of wind vectors, it is crucial to understand how the wind vector components can be derived from the wind speed and direction, in case our measuring device does not output the wind in it's pure vector form. Comparison between wind measurements then requires the proper knowledge of vector calculus, most importantly the addition, subtraction and averaging of vectors.

The addition of vectors can be defined in the following way: To add two vectors

together, we simply add the respective components of the two vectors together. The new vector we get after the addition is then called a resultant vector.

In the case of two two-dimensional vectors $\vec{a}$ and $\vec{b}$, the resultant vector can simply be written as [Galbis and Maestre, 2012]:

$$\vec{a} + \vec{b} = (u_a + u_b)\hat{\imath} + (v_a + v_b)\hat{\jmath} \tag{2.8}$$

Similarly [Galbis and Maestre, 2012]:

$$\vec{a} - \vec{b} = (u_a - u_b)\hat{\imath} + (v_a - v_b)\hat{\jmath} \tag{2.9}$$

Sometimes it is useful to be able to analyze the wind as a combination of wind speed and direction, or simply to be able to analyze and compare one of the two between measurements. In these cases, the length of the vector can be found as following [Galbis and Maestre, 2012]:

$$|\vec{a}| = \sqrt{u^2 + v^2} \tag{2.10}$$

The direction of a wind vector can be found using simple geometry (Figure 2.3):

$$\theta = \arctan\left(\frac{v}{u}\right) \tag{2.11}$$

And meteorological wind direction can be found simply by:

$$DDD = 270 - \theta \tag{2.12}$$

The opposite can also be done; we can easily calculate the vector components, if we know the length and direction of the vector:

$$\vec{a} = (|\vec{a}| \cos\theta)\hat{\imath} + (|\vec{a}| \sin\theta)\hat{\jmath} \tag{2.13}$$

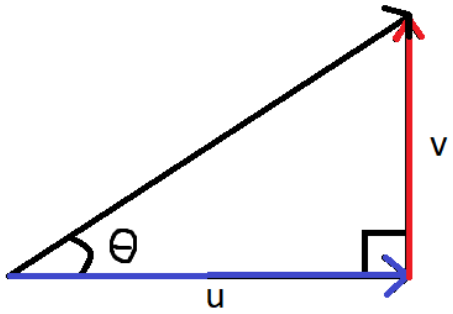

Figure 2.3: Wind vector and its components. Meteorological wind directionn can be found according to equation 2.12

2.4.2 Modular arithmetic

Modular arithmetic is a branch in mathematics, where numbers circle back to zero when a certain integer, called modulus, is reached. Modular arithmetic is present in our everyday lives, most notably in the way our clocks work. In a normal 12-hour clock, the day is divided into 12, hour-long sectors, ranging from 0 to 11. If the time was 4:00, in 9 hours the time would be 1:00, even though a simple arithmetic yields $4+9 = 13$. This is because the numbers circle back to zero at the modulus.

Similarly, if the original wind direction is 300 degrees and the wind then turns 90 degrees clockwise, the new wind direction is 30 rather than 300 + 90 degrees. On the other hand, the absolute difference between the two wind directions is 90 instead of 300 - 30 = 270 degrees.

In this thesis, the concepts of modular arithmetic are used in the analysis of wind direction, most importantly when averaging wind directions over different time periods without the implicit speed weighing caused by taking the mean of the vector components.

This can be achieved by taking the circular mean, which is defined as:

$$\overline{\alpha} = atan2\left(\sum_{i=1}^{n} sin(\alpha_i), \sum_{i=1}^{n} cos(\alpha_i)\right) \tag{2.14}$$

2.4.3 Root mean squared error (RMSE)

Root mean squared error, or from now on RMSE, is often used as an estimator when comparing differences between measurements and reference values. The lower the value of RMSE, the better the measured values compare to the values used as the reference. A RMSE of 0 would imply a perfect agreement between the datasets used [Barnston, 1992].

The mathematical definition of RMSE is quite simple; let's have two time series: $X_{1,t}$ and $X_{2,t}$. Let the first series be the reference and the second be the measured time series. We can define RMSE as following [Barnston, 1992]:

$$RMSE = \sqrt{\frac{\sum_{t=1}^{T}(X_{1,t} - X_{2,t})^2}{T}} \tag{2.15}$$

In this thesis' case, RMSE is used in the analysis of the wind data to make deductions about the measurement accuracy of our measurement arrangement.

2.4.4 Linear regression

In linear regression we assume that there is an underlying linear relationship between the dependent variable (in our case, the reference measurement) and an independent variable (in our case, dronebound measurement). However, there are random errors in the measured values, so that this linear relationship is not cleanly seen in individual pairs of measurements. Linear regression is used to find this underlying relationship by solving the linear least squares relationship between the dependent variable (reference measurement) and independent variable (dronebound measurement) [Galton et al., 1885].

The goal is to find the line of best fit that can accurately predict the values of the dependent variable (Y) based on the values of the independent variables (X). The line of best fit is described by the following equation:

$$\hat{Y} = \beta_0 + \beta_1 X_1 \ ... \ + \beta_n X_n \tag{2.16}$$

We are now working with a case, where there is only one independent variable. The line of best fit reduces to:

$$\hat{Y} = \beta_0 + \beta_1 X_1 \tag{2.17}$$

where the β_0 is the y-intercept and β_1 describes the change in Y in respect to change in X. Now we need to find the aforementioned least squares relationship between Y and X. This can be found by first writing down the equation for sum of squared differences between the predicted and actual values:

$$SSE = \sum_{i=1}^{N}(Y_i - \hat{Y}_i)^2 \tag{2.18}$$

where Y_i is the actual value and $\hat{Y}_i$ is the predicted value from 2.16.

To minimize the sum of the squared differences, we need to find the values of the coefficients that minimize SSE. This can be done by taking partial derivatives respective to β_0 and β_1 and setting them to 0:

$$\begin{aligned} \frac{\partial SSE}{\partial \beta_0} &= 0 \\ \frac{\partial}{\partial \beta_0}\sum_{i=1}^{N}(Y_i - \hat{Y}_i)^2 &= -2\sum_{i=1}^{N}(Y_i - \beta_0 - \beta_1 X_i) = 0 \\ \sum_{i=1}^{N} Y_i - \sum_{i=1}^{N}\beta_0 - \beta_1\sum_{i=1}^{N} X_i &= 0 \end{aligned} \tag{2.19}$$

Now we can find β_0 by solving the equation we got in 2.19:

$$\beta_0 = \overline{Y} - \beta_1\overline{X} \tag{2.20}$$

Now we can repeat the procedure for β_1:

$$\begin{aligned} \frac{\partial SSE}{\partial \beta_1} &= 0 \\ \frac{\partial}{\partial \beta_1}\sum_{i=1}^{N}(Y_i - \hat{Y}_i)^2 &= -2\sum_{i=1}^{N} X_i(Y_i - \beta_0 - \beta_1 X_i) = 0 \end{aligned} \tag{2.21}$$

Now we can substitute the value of β_0 and with simple arithmetic, we can find β_1:

$$\beta_1 = \frac{\sum_{i=1}^{N}((X_i - \overline{X})(Y_i - \overline{Y}))}{\sum_{i=1}^{N}(X_1 - \overline{X})^2} \tag{2.22}$$

3. Measurements and data

3.1 Measurements

The measurements for this thesis were conducted in Jokioinen, Finland between 2nd of September and 10th of October 2022. Overall 20 sets of measurements were conducted, consisting of fourteen stationary wind measurements and six vertical wind profile measurements. Together these add up to around 440 minutes of measurement time.

The stationary wind measurements were conducted by first flying the drone next to the wind mast anemometer used as a reference, which is located 30 metres above ground level (AGL from now on). The drone was then headed towards compass north by the help of the GPS signal from the drone. The effect of magnetic declination was included in the analysis. This introduces a source of possible human error, as the direction has to be approximated and thus might sometimes be not completely northward. After the drone is at the proper height and location, the measurement can begin. Wind is then measured as long as the drone has batteries. After critical battery level is reached, the drone is safely landed and measurement ends. Data points from the landing period are removed from the analysis, as they would skew the results.

The vertical wind profile measurements are conducted by using the drone's autopilot feature. The autopilot is programmed to first rise to the AGL height of 30 metres and hover for a time period of 30 seconds. After the hovering period, the drone then rises to 50 metres, and hovers for another 30 seconds. This is thereafter repeated every 50 metres AGL, until 500 metres AGL is reached. At 500 metres, the last hovering period is conducted, and then the drone descends and lands. For the wind analysis, the measurements during the hovering periods are averaged and then compared with automatic radiosoundings.

3.2 Data

Anemoment Trisonica Mini Wind and Weather Sensor produces high quality data of all the most important atmospheric variables, including temperature, humidity, as well as wind speed and direction. The most important specifications concerning wind measurements are given in table below (Table 3.1):

Parameter	Value
Sampling frequency	1 Hz
Wind speed range	0-50 m/s
Wind speed resolution	0.1 m/s
Wind speed accuracy	(0-10 m/s) ± 0.1 m/s; (11-30 m/s) ± 1%
Wind direction range	(x,y) 0-360°; (z) 0-30 °
Wind direction resolution	1 °
Wind direction accuracy	±1°

Table 3.1: Relevant specifications of Anemoment Trisonica Mini Wind and Weather Sensor.

As a reference measurement, we used Adolf Thies GMBH & CO.KG Ultrasonic Anemometer 2D. The operating principle is similar to that of the Anemoment Trisonica Mini Wind and Weather Sensor, and specifications are also comparable (Table 3.2):

Parameter	Value
Sampling frequency	1 Hz - 1 kHz
Wind speed range	0.01-75 m/s
Wind speed resolution	0.1 m/s
Wind speed accuracy	(0-5 m/s) ± 0.1 m/s; (>5 m/s) ± 2%
Wind direction range	(x,y) 0-360°
Wind direction resolution	1 °
Wind direction accuracy	±1°

Table 3.2: Relevant specifications of Adolf Thies GMBH & CO.KG Ultrasonic Anemometer 2D.

Overall the specifications of the two anemometers are almost the same, the only notable difference being the slightly better accuracy of Trisonica Mini Wind and Weather Sensor at wind speeds over 5 m/s.

3.3 Measurement arrangement

The UAV used as a measurement device chassis was DJI Matrice 600 Pro (M600P henceforth). M600P is an hexacopter with dimensions of 1668 mm × 1518 mm × 727 mm with propellers, frame arms and GPS mount unfolded (including landing gear) and 437 mm × 402 mm × 553 mm with propellers, frame arms and GPS mount folded (excluding landing gear). With starting weight of 9.5 kg - 10 kg depending on the battery package used, and with capability of lifting payloads up to 6 kilograms, M600P is more than adequate for wind measurements. Below a schematic figure of the measurement arrangement can be found (Figure 3.1):

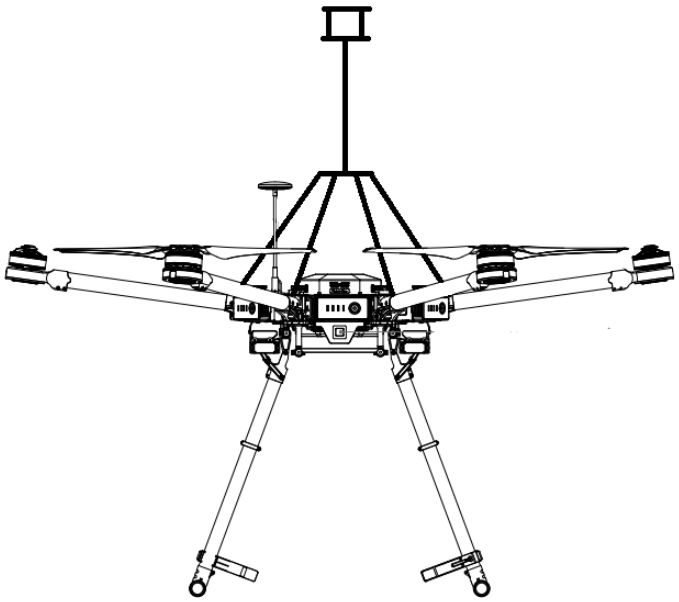

Figure 3.1: Schematic figure of the measurement arrangement. Total dimensions with anemometer and quadropod attached is 1668 mm × 1518 mm × 1487 mm with propellers, frame arms and GPS mount unfolded. The hollow box on top of the pole marks the placement of the anemometer. Original schematic from Matrice 600 Pro User Manual.

4. Results

In the following sections, we will be going through the results of the analysis of our wind data. We will first discuss the stationary wind measurements and then the vertical wind profiles. After they have been gone through, we will compare our results with selected earlier studies.

When talking about differences between reference and dronebound measurements, the subtraction has always been made from the drone measurement, i.e. $\Delta X = X_{Drone} - X_{Reference}$. Min and max values in tables correspond with absolute minimum and maximum values of the analyzed datasets.

4.1 Stationary wind measurements

4.1.1 Qualitative analysis of wind roses

A as summarisation of the stationary wind measurements, a wind rose of all the available data for both measurements, averaged to 10 minute periods, is shown in figure 4.1.

Even though the wind distributions look different from each other, they have some characteristics they share. The dronebound as well as the reference measurement agree on the fact the most prominent wind directions are roughly from East and South. The distributions having emphasis on Southerly and Easterly winds probably yields from the rather small amount of measurements.

The difference is that the direction distribution in the dronebound measurements seems to be rather more extreme; where the reference measurement has measured winds from East and East Southeast, the dronebound anemometer has measured almost only East winds. Similarly for the southerly direction wind measurements: dronebound anemometer has measured mostly winds coming from South, where the reference measurement clearly shows winds also from South Southwest.

The wind distributions looking different makes the qualitative analysis of them rather difficult. Notably, the East winds seem to be in closer agreement between the dronebound and reference measurement. The magnitudes of the wind speeds and the number of measurements in each bin are in quite good order. When comparing the Southern sector of wind measurements, we see larger differences, as the magnitudes seem to differ a lot more between the measurements. The 3.0 - 4.0 m/s bin is underrepresented in the dronebound measurement, as well as a small bin of >6.0 m/s wind speed can be found in the dronebound wind rose, which is not present on the reference wind rose. The wind roses would lead us to believe that the dronebound anemometer has positive bias in wind speed, at least in the Southerly direction.

Overall the qualitative analysis of wind roses does not tell us the whole truth, and a deeper quantification is needed, as the bin-like structure of wind roses can easily lead one astray. The measured wind directions can differ as little as 1° and end up in different sectors, as the rose consists of 16 22.5° sectors.

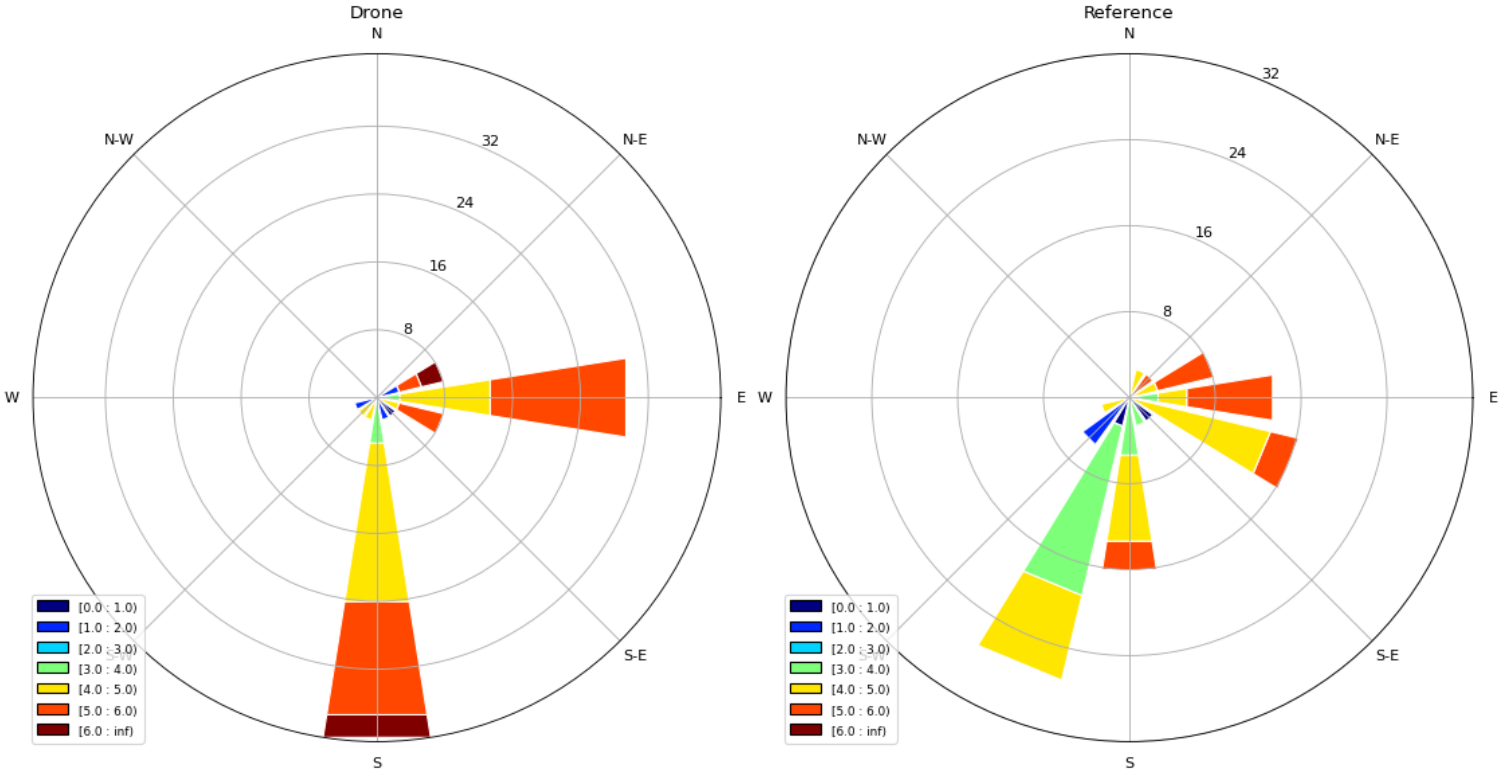

Figure 4.1: Wind roses of dronebound anemometer (left) and reference anemometer (right). Note the difference in scales.

4.1.2 Wind speed analysis

In Figure 4.2 below, we have a typical set of wind speed measurements from September 2, 2022, which will also be used for illustration in some of the later figures. At the beginning of the dataset, the wind speeds differ quite a lot, but this disagreement does not last long. Between 10:23 and 10:27 we can see a period in which the reference and dronebound measurements are in almost complete agreement. Overall the measurements seem to agree quite well: the difference seems to be less than 10% of the magnitude of the reference measurement, except in the beginning and in the end.

The overall trends of the measurements are also in order: the dronebound wind speed seems to grow when the reference wind speed grows, and similarly it decreases as the reference wind speed is decreasing.

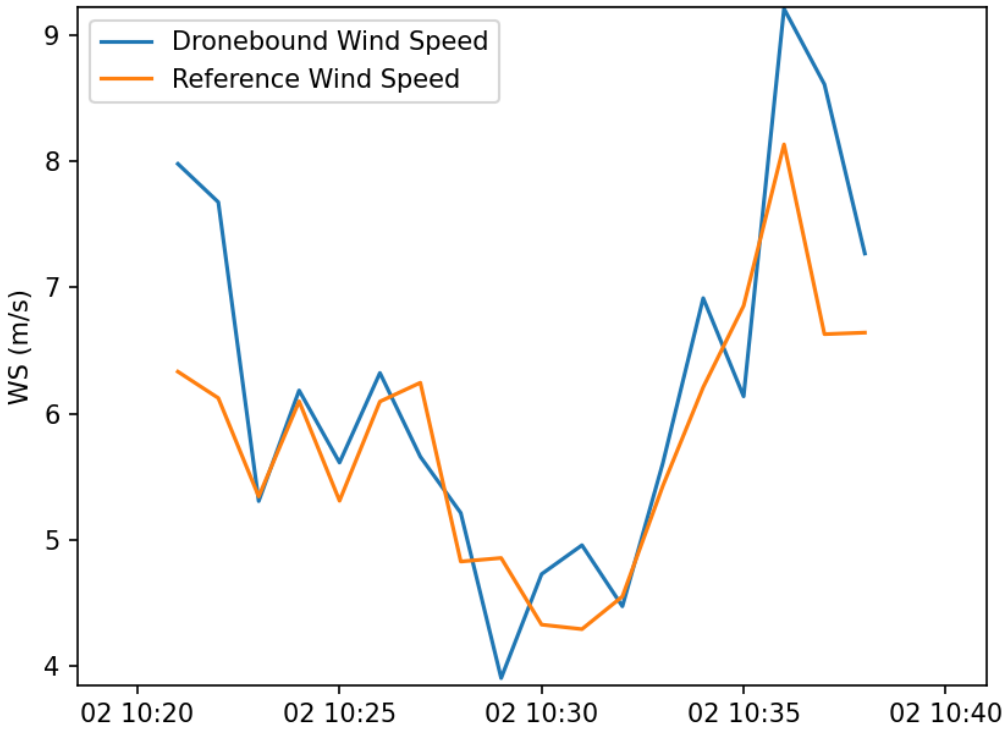

Figure 4.2: 1 minute wind speed averages on 02.09.2022.

Next we will be discussing the statistics of the wind speed measurements. In Table 4.1, the key statistics for the stationary wind speed results are shown:

	Wind speed, reference (m/s)	Wind speed, drone (m/s)	Difference (m/s)
mean	4.120	4.456	0.336
std	1.268	1.396	0.674
min	0.522	0.742	-1.313
25%	3.889	4.068	-0.060
median	4.237	4.817	0.220
75%	4.898	5.327	0.579
max	5.897	6.437	1.991

Table 4.1: Key statistics of the 10 minute averages of the stationary wind speed measurements. The difference column has been calculated from the differences of measurement pairs.

As we can see from the statistics, the mean and median values are quite close to each other. The mean difference between the reference and dronebound measurement is less than 10%, which is considered sufficient by WMO standards. Even the 25% and 75% are very close to each other, with the third quartile having a larger difference between the measurement pairs.

The skewness of the results is also notable. As we can see from the difference column in table 4.1, the mean and median difference have a significant difference, with the mean being about 0.12 m/s greater. This would imply that the wind speed difference distribution is skewed to the right, though with small sample size this can be caused by simply random variation. In figure 4.3 the distribution of the wind speed difference is plotted.

From the Kernel density estimation plot we can see that the wind speed differences are mostly positive, which implies that the wind speeds measured by the dronebound anemometer are higher. If that is the case, we should be able to see it also in a regression plot. Thus below in figure 4.4 we have the wind speed regression plot.

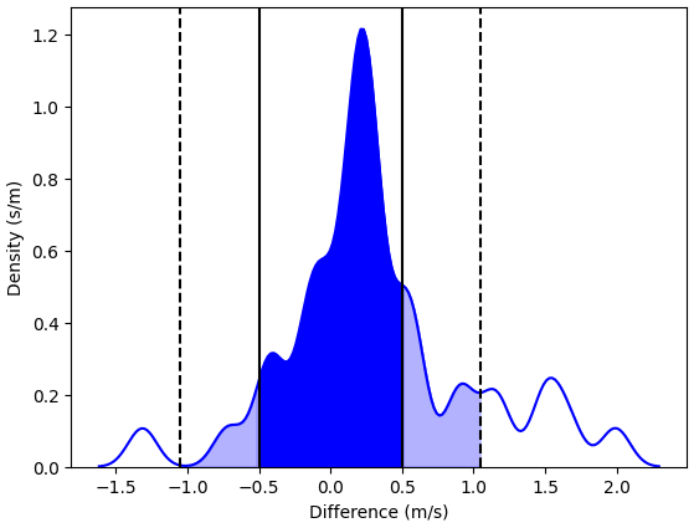

Figure 4.3: Kernel density estimation of the differences in wind speed. Solid black lines mark the 0.5 m/s difference (WMO standardisation) and the dashed black lines mark the 1/10th of the maximum wind gust in the dataset.

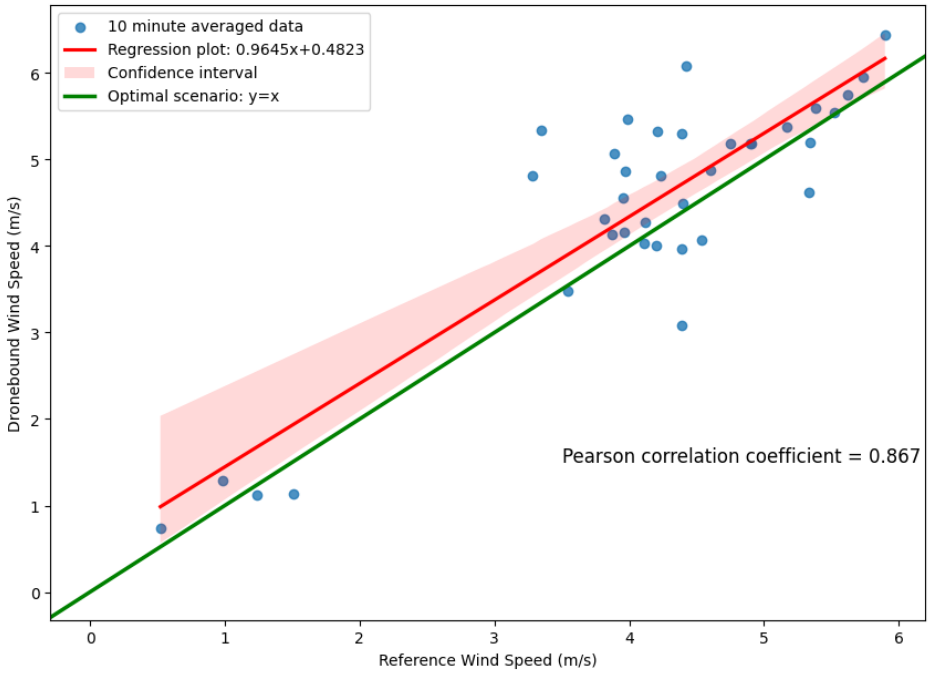

Figure 4.4: Regression plot of the dronebound wind speed against the reference wind speed

The regression plot 4.4 validates what we already deduced before, but also gives us the formula for the linear relationship between the dronebound (y) and reference (x) measurements. In our case it is:

$$y = 0.9645x + 0.4823 \tag{4.1}$$

which implies, that there is positive bias in the dronebound measurement.

The linear relationship between the reference and dronebound measurement is not exactly the optimal case of perfect linear relationship, in which $y = x$, but we are sufficiently close. The constant term is within the WMO standardisation for wind speed (0.5 m/s under wind speed of 5 m/s, 10% of wind speed when WS $>$ 5 m/s) and the slope is only off 3.55% of the optimal case.

Before moving on to wind direction analysis, we will shortly discuss the RMSE of our wind speed measurements. In Table 4.2 below, RMSEs for all the days measurements were conducted on, and for all the data sets as a whole, are shown:

Date	Number of 10 minute averages	RMSE (m/s)
02.09.2022	3	0.393
07.09.2022	3	0.302
15.09.2022	6	0.972
22.09.2022	6	0.273
27.09.2022	12	0.217
05.10.2022	12	1.140
All datasets	42	0.745

Table 4.2: RMSE values for wind speed measurements.

As we can see, the RMSE vary from about 0.22 m/s to over 1.1 m/s. Overall the RMSEs are of expected magnitude. The exceptions are the datasets from 15th of September and 5th of October. This is probably because of either a GPS signal problem, which would cause the drone to be unable to stay stationary in the air, or simply because of stronger wind gusts, which might have caused the drone to compensate for the wind more than normally, leading to the anemometer starting to shadow itself, causing errors in the measurement. On 5th of October slight precipitation also occurred during the measurement period, which might have negatively affected the quality of the measurement, leading to decreased measurement accuracy.

Overall the RMSE values are inline with previously conducted similar studies. Comparisons with the results of previous studies will be discussed in section 4.3.

4.1.3 Wind direction analysis

In Figure 4.5 below, we have a typical set of wind direction measurements. Wind direction is more susceptible to the limitations set by the measurement arrangement, including errors caused by weak or momentarily lost signal. Also the turbulent nature of surface layer winds causes some inaccuracies with wind direction measurements.

As we can see from Figure 4.5, the measurement starts with reference and dronebound anemometers in a good agreement. At around 10:26, the measurements disagree significantly for a moment. A reason for this behaviour is hard to pinpoint, but an eddy that was only measured by the dronebound anemometer is a possibility. After 10:26, the measurement continues with both anemometers in good agreement.

The overall trend of the measurements is in order: the dronebound wind direction seems to increase when the reference wind direction increases, and similarly it decreases as the reference wind direction is decreasing.

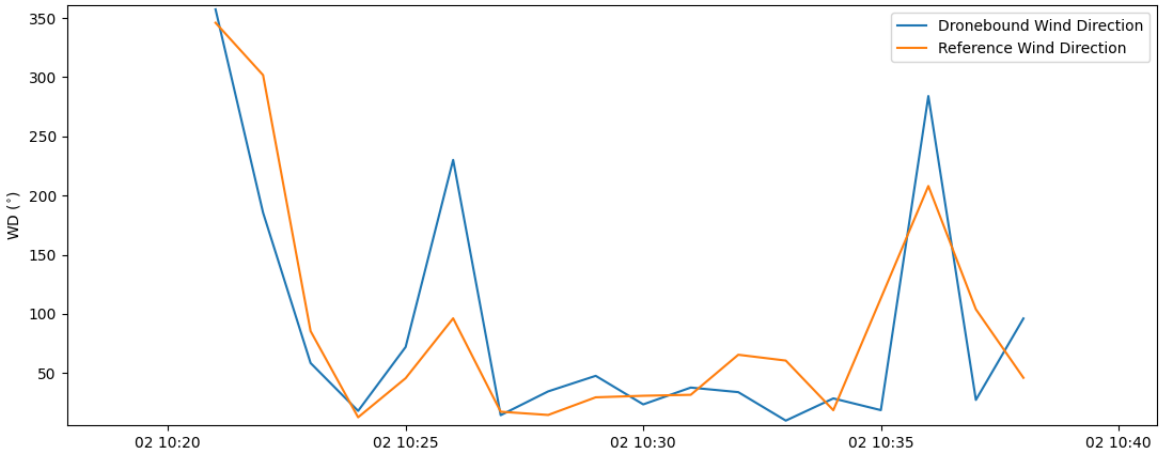

Figure 4.5: 1 minute wind direction averages on 02.09.2022.

Next we will discuss the most important statistics of the wind direction measurements. In Table 4.3 they key statistics for the stationary wind direction measurements are shown:

	Wind direction, reference (°)	Wind direction, drone (°)	Difference (°)
mean	147.965	140.723	-7.242
std	58.100	51.822	12.187
min	33.485	56.625	-58.366
25%	98.827	91.846	-11.463
median	175.286	160.707	-4.736
75%	194.099	181.713	-0.029
max	252.566	244.701	25.514

Table 4.3: Key statistics of the 10 minute averages of the stationary wind direction measurements. The difference column has been calculated from the differences of measurement pairs.

As we can notice from the statistics, the mean and median of the wind direction difference differ by about 2.5°. Both are also negative, implying that the wind direction measured by the dronebound anemometer is negatively, or counter clockwise, biased. This is also imminent if we look at the third quartile; the negative value of the third quartile implies that the distribution of differences in wind direction is mostly negative, with less than 25% of the differences being positive. In Figure 4.6, the distribution of the differences is shown:

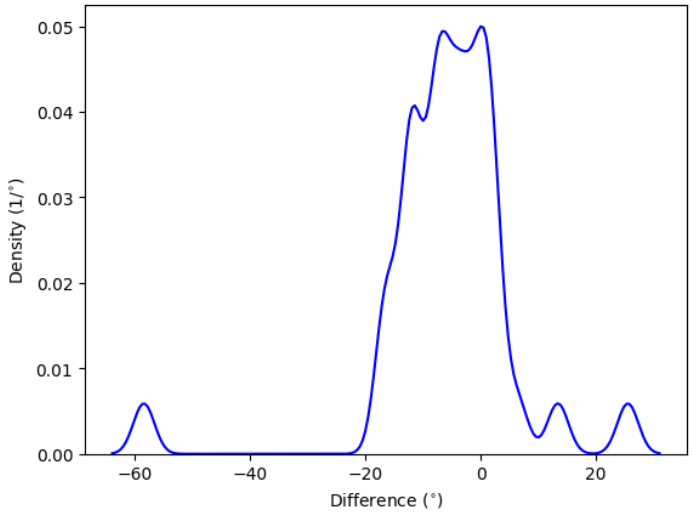

Figure 4.6: Kernel density estimation of the differences in wind direction.

As we can see, the difference distribution is mostly concentrated between -20 ° and 10 °, with 75.6% of the differences being negative.

Next we will take a look at the RMSE for our wind direction measurements. In Table 4.4 below, RMSEs for all the days measurements were conducted on, and for all the data sets as a whole, will be shown:

Date	Number of 10 minute averages	RMSE (°)
02.09.2022	3	1.586
07.09.2022	3	6.092
15.09.2022	6	7.608
22.09.2022	6	29.643
27.09.2022	12	9.146
05.10.2022	12	12.307
All datasets	42	13.300

Table 4.4: RMSE values for wind direction measurements.

The RMSEs are of similar magnitude and mostly inline with each other. On 2nd of September the RMSE has been about an order of magnitude smaller than on other days of measurement. This yields purely from the small amount of data from that day, with only three 10 minute observations.

On the other hand, on 22nd of September, the RMSE of the wind direction is abnormally high; this supports the hypothesis of GPS signal problems having occurred on the 22nd, as nothing else explains such a large difference between the 22nd and other days of measurement.

Overall the RMSEs are inline with earlier studies. Comparisons to previous studies will be discussed in depth in section 4.3.

4.1.4 Wind vector analysis

In Figure 4.7 below, we have the wind vector components from the set of measurements that was used earlier in Figs. 4.2 and 4.5. As we can see, the agreement is overall pretty good. There is some disagreement in the measurements at the very beginning, but from around 10:23 forwards the reference anemometer and dronebound anemometer measure similar values for both wind components.

The temporal variations in the dronebound and reference measurements are also in agremeent. The U and V winds from the dronebound measurements increase simultaneously with the reference measurements, and similarly U and V from the dronebound measurements decrease when they decrease in the reference measurements.

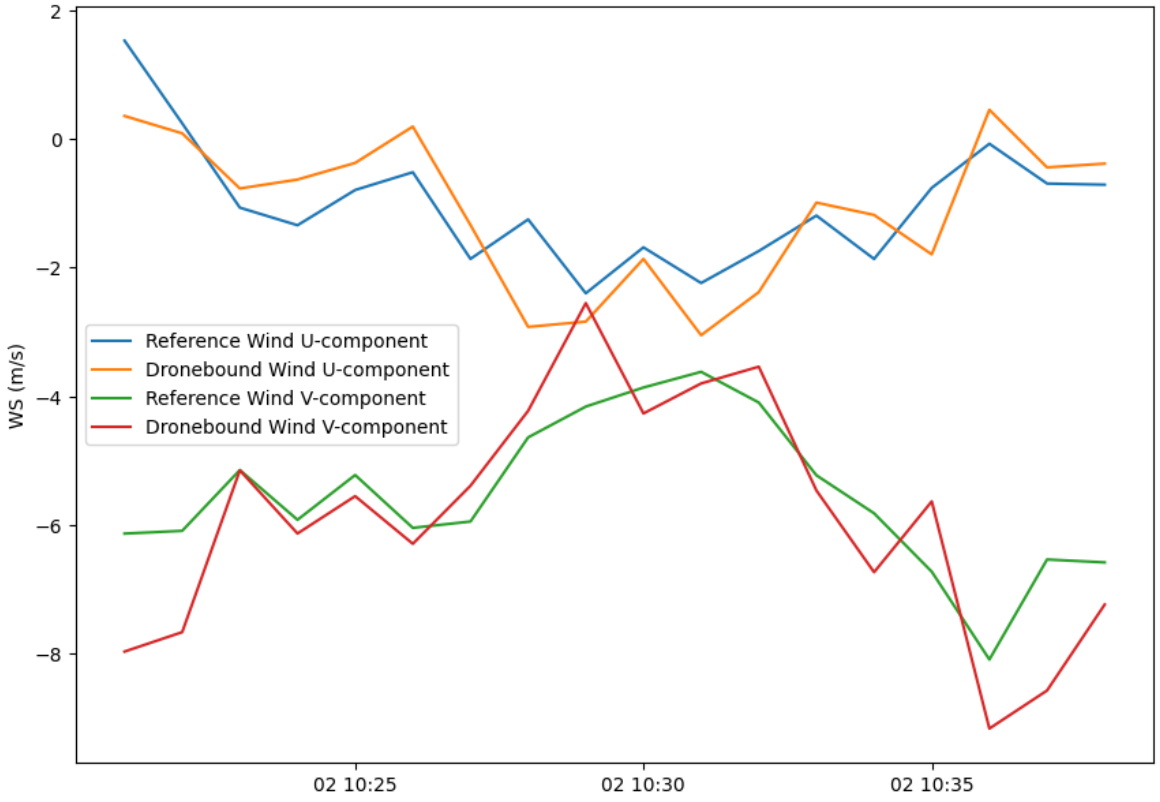

Figure 4.7: 1 minute wind vector component averages on 02.09.2022.

Next we will be discussing the statistics of the measured wind components. The key statistics are shown in Table 4.5 below:

	U-component difference (m/s)	V-component difference(m/s)	Vector difference (m/s)
mean	-0.124	0.029	0.894
std	0.527	0.950	0.614
min	-1.799	-1.580	0.045
25%	-0.396	-0.537	0.445
50%	-0.044	0.005	0.792
75%	0.106	0.557	1.171
max	0.869	2.129	2.394

Table 4.5: Key statistics of the 10 minute averages of the stationary wind vector measurements.

We can see that the vector differences are quite large, implying that the combined effect of wind speed difference and direction difference are significant.

Overall the mean and median differences are close to zero for both wind vector components.

Next we will take a look at the distributions of the differences between the reference and dronebound measured wind vector components. They are shown in figure 4.8.

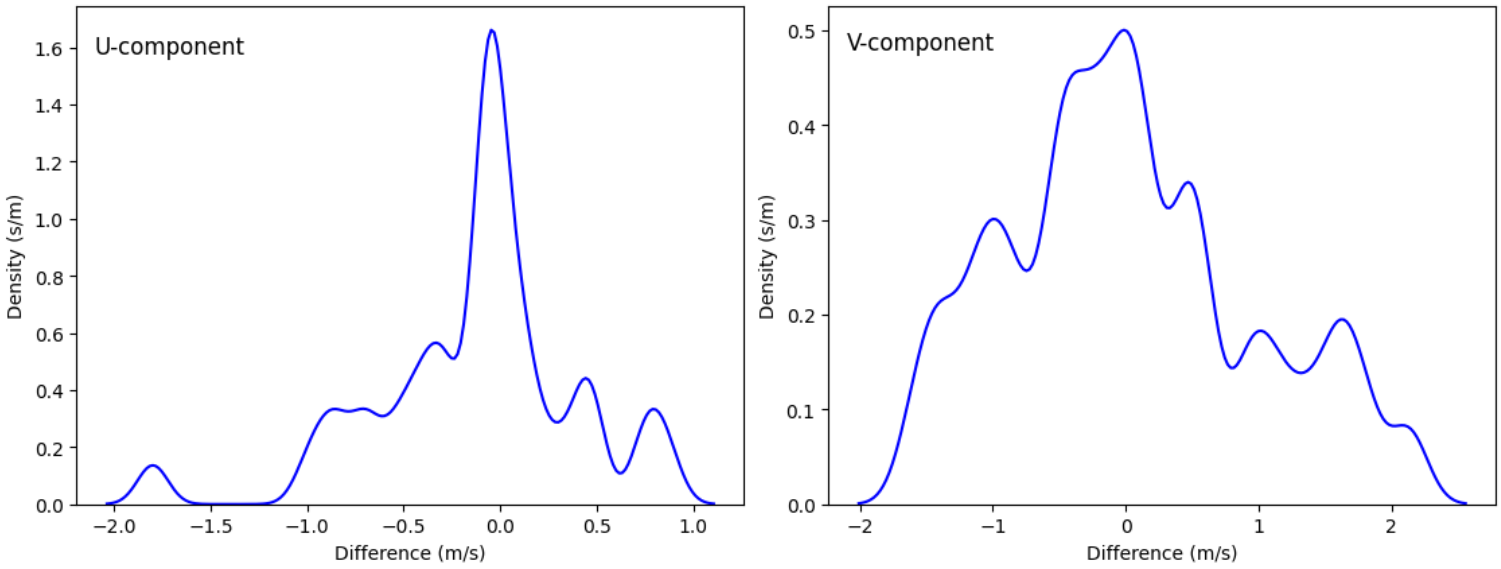

Figure 4.8: Distributions of differences between the drone-measured and the reference wind vector components

From the distributions we can notice something that could be noticed by comparing

the standard deviations of the measurements; the measurement of U-component of the wind vector has actually been better than that of the V-component. This we can see from the shape of the distributions. The U-component differences have a clear spike within the [-0.25 ; 0.25] region, which implies that large fraction of the calculated difference data points are in this region. The V-component differences do not have such a spike; the distribution resembles that of a Gaussian distribution, implying the greater variance of the measurement already discussed beforehand. Overall the V-component distribution is wider at [-2.5 ; 2] m/s, whereas U-component varies between [-2.0 ; 1.2] m/s.

Next we will be taking a look at the RMSE values of our wind vector components. In Table 4.6 RMSEs are shown for each day of measurements separately and for the whole data set, for each of U and V separately:

Date	RMSE, U (m/s)	RMSE, V (m/s)	RMSE, Wind vector (m/s)
02.09.2022	0.060	0.305	0.311
07.09.2022	0.589	0.323	0.672
15.09.2022	0.470	1.009	1.113
22.09.2022	0.923	0.823	1.237
27.09.2022	0.212	0.780	0.809
05.10.2022	0.616	1.259	1.402
All datasets	0.535	0.938	1.08

Table 4.6: RMSE values for wind vector components.

The RMSEs for the U-component are overall smaller than for the V-component. This is mostly because of the larger variance of the V-component differences. We also notice that the V-component RMSEs are much higher than the wind speed RMSEs found in Section 4.1.2. U-component RMSEs are instead comparable to the wind speed RMSEs. All in all the RMSEs of U-component are of similar magnitude to earlier studies, with V-component RMSEs being higher.

And lastly we will have the difference vectors shown below in Figure 4.9, to visualize the differences in wind speed and direction as a whole.

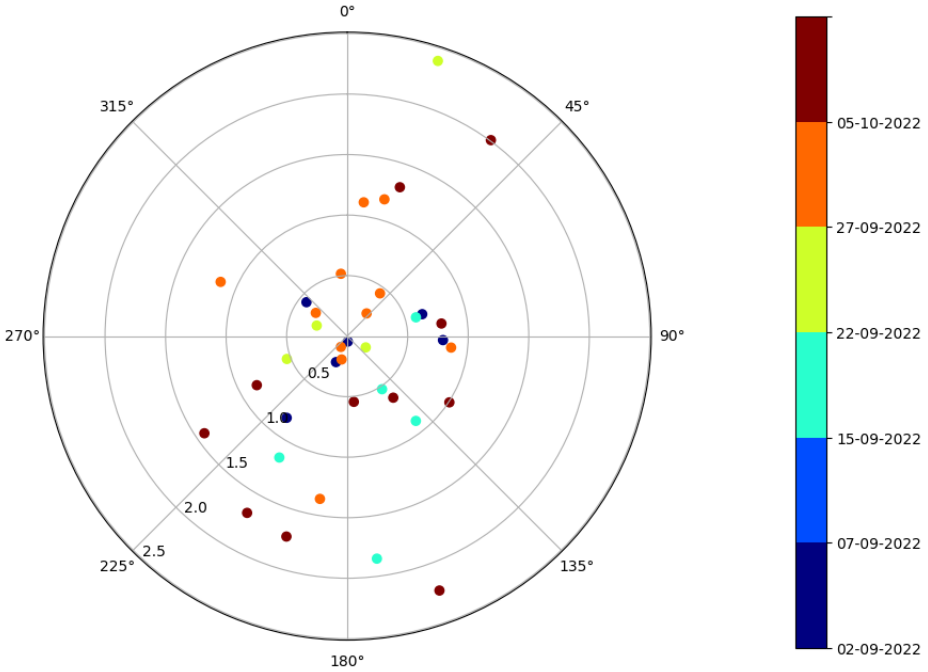

Figure 4.9: Difference between drone-measured and reference wind vector components.

4.2 Wind profiles

In this section the results of the analysis on the vertical wind profiles will be gone through. But before we can discuss the actual results, we need to look at the difficulties in the analysis.

As we analyze the vertical wind profiles, we are actually comparing the instantaneous wind vectors measured by the automatic radiosounding to the dronebound wind measurements. The difficulty lies in the fact that we cannot conduct the measurement at the very same time as the radiosounding, as that could lead to a potentially dangerous situation if the radiosonde and drone would come in contact with each other. Because of that, our reference measurement and dronebound measurement have a slight time difference between each other.

A second problem is the fact that the radiosounding used as a reference does not actually rise straight up, but instead moves with the wind. Our drone setup of course rises straight up, without ever changing it's coordinates. This causes a slight spatial difference in the measured winds.

The third and the last problem is the fact that the drone measures mean winds during short hovering periods. Meanwhile the wind data from the radiosounding is calculated independently based on satellite carrier frequency changes every 2 seconds. This means that we are comparing 30 second averages to almost instantaneous wind data. Thus the differences can get quite high.

4.2.1 Wind speed analysis

We will first analyse the wind speed profiles. Wind speed profile measured on 2nd of September 2022 is shown in Figure 4.10 below:

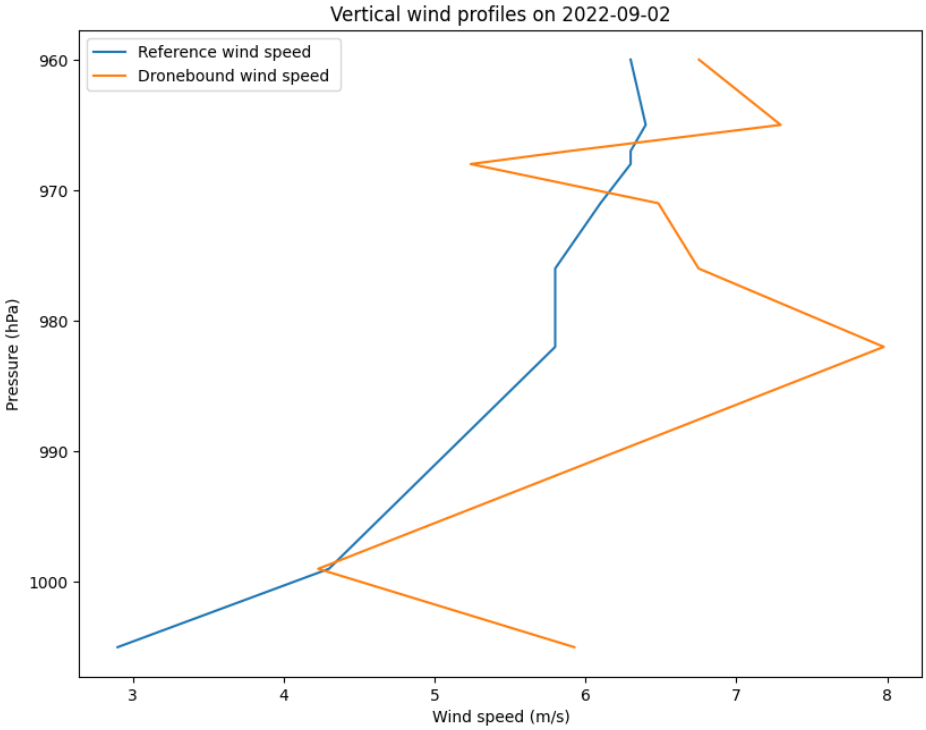

Figure 4.10: Wind speed profile on 02.09.2022

As we can see, the wind speeds do not correlate very well. The difference between reference and dronebound measurements seems to fluctuate randomly. The measured wind speeds are close to each other only on one pressure level. The difference in the profile might be caused by the automatic radiosounding passing through the air layer faster than the drone. Thus the wind speed would have had less time to change. Another possible reason is noise caused by the random measurement errors.

From measurement differences this large and random, it's hard to say anything conclusive. Next we will look at the key statistics of the wind speed profile measurement, which are shown in Table 4.7 on the next page.

	Wind speed, reference (m/s)	Wind speed, drone (m/s)	Difference (m/s)
mean	5.948	6.456	0.508
std	2.589	2.531	1.423
min	0.900	1.085	-4.360
25%	4.600	5.060	-0.184
median	5.750	6.395	0.425
75%	7.275	7.447	1.270
max	11.700	12.005	3.027

Table 4.7: Key statistics of the wind speed profile measurements. The difference column has been calculated from the differences of measurement pairs.

From the statistics one feature is imminent: the quality of the profile measurements has not been as good as the quality of the stationary wind measurement. The shorter measurement time compared to stationary measurements lowers the accuracy. We also need to remember that even a perfect drone measurement wouldn't yield exactly same results as the radiosounding because of the slight time difference between the measurements.

The key statistics, including the mean difference, standard deviation of measurement pair differences and the median difference are all larger than the respective stationary measurement statistics. The larger standard deviation also implies that the RMSEs for the profile measurements are larger than the stationary measurements.

Before discussing RMSEs for the wind speed profiles, we will look at the regression and correlation of the wind speed profile measurements. These are shown on Figure 4.11 on the next page.

From Figure 4.11 we can easily see that both the regression line and Pearson's correlation coefficient are further from the optimal situation than in the case of stationary wind measurements. Pearson correlation coefficients are overall closer to each other between the different measurement types than the slopes of regression plots are.

Next we will look at the RMSEs of the wind speed profile measurements. These are shown in Table 4.8 on the next page.

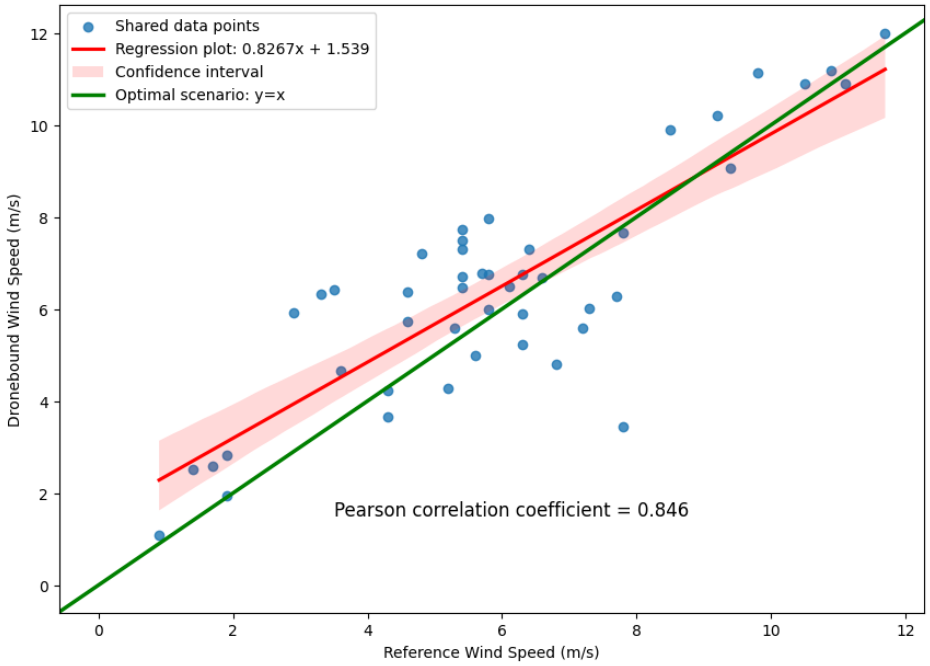

Figure 4.11: Regression plot and Pearson's correlation coefficient for wind speed profile measurements.

Date	RMSE (m/s)
02.09.2022, only set	1.385
07.09.2022, first set	2.595
07.09.2022, second set	1.573
15.09.2022, only set	1.627
22.09.2022, only set	0.765
27.09.2022, only set	0.937
All datasets	1.495

Table 4.8: RMSE values for wind speed profile measurements. On all days but 7th of September a single wind profile measurement was conducted. On 7th of September two sets were conducted instead.

From Table 4.8 we can easily see the fact that RMSEs are higher for the profile measurements than for the stationary measurements. For all the datasets the ratio between profile and stationary measurements is 2.01, implying that the value of typical error is 2.01 times larger for profile measurements.

4.2.2 Wind direction analysis

In Figure 4.12 vertical profile of wind direction is shown for the measurements made on September 2, 2022:

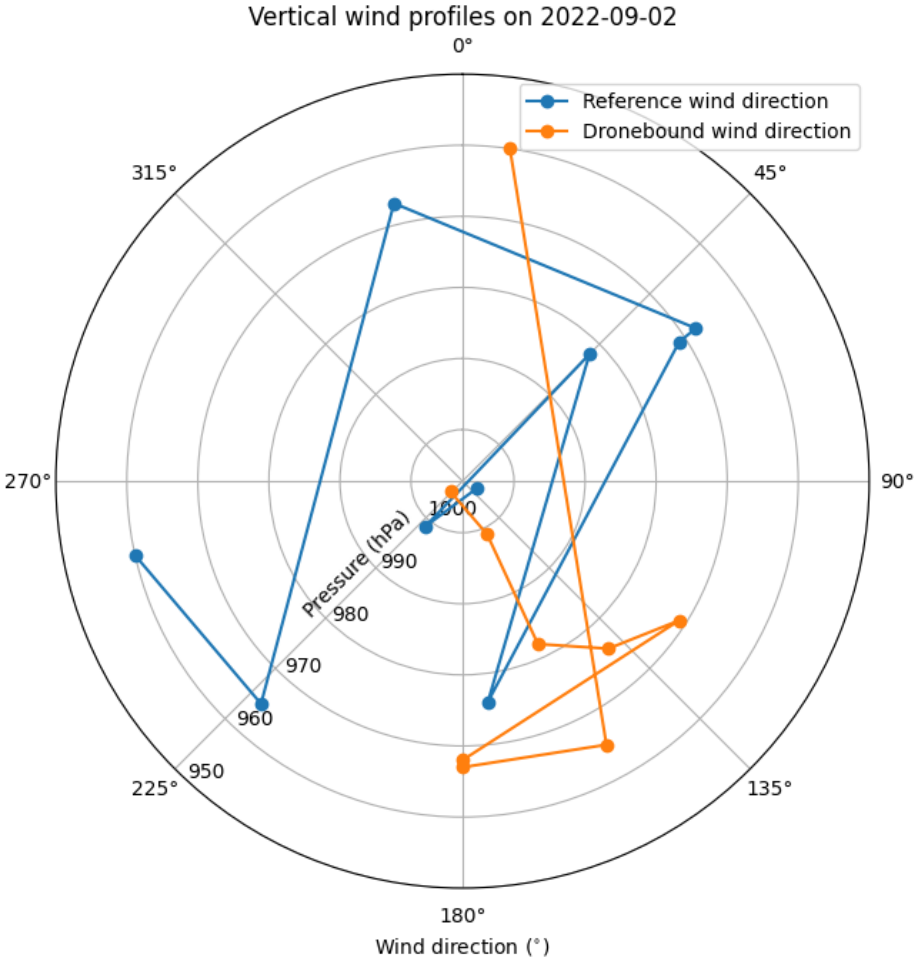

Figure 4.12: Wind direction profile on 02.09.2022.

As we can see from the figure, there is quite a large disagreement with the wind directions. This is expected, due to the temporal difference between the measurements, as well as the fact that we are comparing instantaneous wind directions to 30 second averages. Turbulence can affect the wind direction drastically in the boundary layer.

In Table 4.9 key statistics for wind direction in profile measurements is shown. Notably the mean difference is now positive, when in stationary measurements it was negative.

	Wind direction, reference (°)	Wind direction, drone (°)	Difference (°)
mean	170.304	183.198	12.894
std	113.052	114.435	19.632
min	14.000	0.786	-68.000
25%	113.250	113.569	-21.401
median	168.000	173.062	-7.451
75%	243.750	297.691	0.581
max	355.000	355.688	26.000

Table 4.9: Key statistics of the profile measurements of wind direction . The difference column has been calculated from the differences of measurement pairs.

Next we will look at the RMSEs for the wind direction in profile measurements. The RMSEs are shown in Table 4.10 below:

Date	RMSE (°)
02.09.2022, only flight	15.292
07.09.2022, first flight	33.467
07.09.2022, second flight	27.451
15.09.2022, only flight	17.303
22.09.2022, only flight	31.277
27.09.2022, only flight	8.788
All datasets	22.115

Table 4.10: RMSE values for wind direction profile measurements.

As in previous cases, we once again see that the RMSE are overall significantly higher for profile measurements than for the stationary measurements. RMSEs of datasets from the 2nd and 27th of September are inline with the stationary measurements, but otherwise the RMSEs are larger.

4.2.3 Wind vector analysis

In Figure 4.13 the wind vector components as a function of pressure are shown:

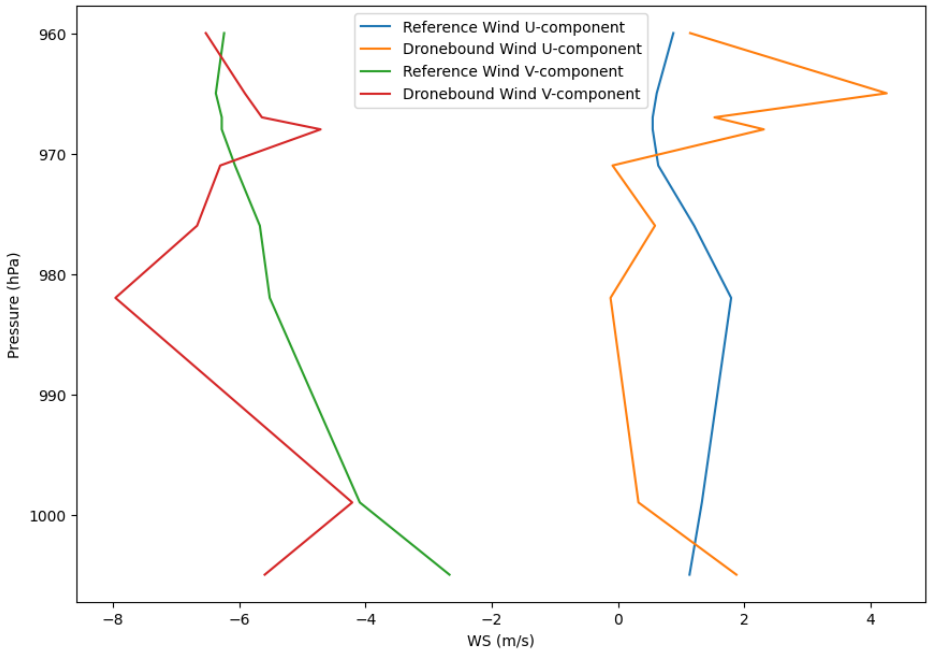

Figure 4.13: Wind vector components as a function of pressure on 02.09.2022.

The agreement between the measurements varies from decent to not very good. The agreement in this case (September 2, 2022) seems to be the best around 970 hPa pressure level.

Statistics for the vertical profiles of wind vector differences are shown in Table 4.11 below. Unsurprisingly, we notice the same thing as before; the main statistics are all worse for the vertical profiles than for equivalent stationary measurements.

A surprising feature is the fact that now the v-wind components measurement seems to have been better than that of the u-component. This is most likely caused by pure chance, but the possibility of stronger winds affecting the measurement in unexpected ways can't be outright refused. Sadly with the data available we can only speculate.

The vector difference column shows a significant difference between the drone measured wind vectors and reference wind vectors. Unsurprisingly the mean and median vector differences are about three times larger than for the stationary wind measurements.

In Table 4.12 RMSEs for each component are shown separately, as well as for the datasets as a whole:

	U-component difference (m/s)	V-component difference (m/s)	Vector difference (m/s)
mean	0.190	-0.193	1.958
std	1.804	1.383	1.148
min	-3.334	-2.926	0.182
25%	-1.005	-1.050	1.082
50%	0.194	-0.130	1.791
75%	1.017	0.661	2.758
max	4.358	2.925	4.779

Table 4.11: Key statistics of the wind vector profile measurements. The difference column has been calculated from the differences of measurement pairs.

Date	RMSE, U (m/s)	RMSE, V (m/s)	RMSE, Wind vector (m/s)
2022-09-02, only flight	1.616	1.443	2.167
2022-09-07, first flight	2.575	3.164	4.080
2022-09-07, second flight	2.909	1.421	3.238
2022-09-15, only flight	1.646	1.552	2.262
2022-09-22, only flight	0.745	0.947	1.205
2022-09-27, only flight	1.267	1.281	1.802
All datasets	1.893	1.671	2.526

Table 4.12: RMSE values for wind vector components.

As expected, the RMSEs for the wind components of the vertical profile are higher than the RMSEs of the equivalent stationary measurements. Normally this would tell us that the measurement quality of the stationary measurements is higher, but as our reference measurement is not ideal for the vertical profiles, we cannot outright prove the difference in quality of the measurements.

4.3 Comparison to previous studies

For the comparisons to the previous studies, the focus will be on the stationary measurements. The comparisons will be based on the mean differences as well as RMSE-values. Our results will be compared with three different earlier studies with similar aims as ours.

4.3.1 Comparison of results with [Palomaki et al., 2017]

In their research, *Palomaki et al.* used similar, yet different setup to the one we ended up using. They utilized a smaller hexacopter with 550 millimeter motor to motor diameter frame (DJI Flame Wheel F550). The anemometer of their choice was a 500 gram 2D sonic anemometer (Decagon Devices DS-2), which was attached to the copter with 30 centimeter pole. Overall the setup was smaller, with a lot heavier payload. They logged instantaneous wind data with 1 Hz frequency. *Palomaki et al.* had also subtracted the bias caused by propeller downwash from their results. They also applied two different methods of measurement, direct (anemometer attached) and indirect (calculating wind information from IMU data). For comparison purposes we will be using the results of the direct method.

In Table 4.13 the comparisons between bias and RMSEs of their and our results:

	Wind speed (m/s), *Palomaki et al.*	Wind speed (m/s), our results	Difference (m/s)
Bias	0.0775	0.336	-0.2585
RMSE	[0.27 ; 0.67]	0.745	[-0.475 ; -0.075]
	Wind direction (°), *Palomaki et al.*	Wind direction (°), our results	Difference (°)
Bias	8.75	-7.242	15.992
RMSE	[29 ; 56]	13.3	[15.7 ; 42.7]

Table 4.13: Comparison of our results and results of *Palomaki et al.*. The difference column shows the difference of values shown in the first two columns, in such way that $\Delta X = X_{Palomaki} - X_{OR}$

Firstly, we can deduce our wind speed biases are nearly an order of magnitude higher than that of *Palomaki et al.*. This is most likely because of the fact they filtered out the bias caused by propeller downwash from their data.

Secondly, even though our wind speed bias was higher, the wind speed RMSEs do not deviate as much. *Palomaki et al.* acquired RMSEs between [0.27 ; 0.67] (m/s) for their

wind speed measurement, meaning that our RMSE of all available data is comparable to their worst dataset, and significantly higher than their best. This would imply that our measurement setup is slightly worse from the measurement quality point of view when it comes to wind speed measurement.

Thirdly, the absolute value of the bias of wind direction is comparable between our measurement and that of *Palomaki et al.*. The sign of the bias is just different, meaning that their setup overestimated the wind direction, whereas our underestimated it.

Fourthly and lastly, the RMSEs of wind direction. Here we can see the largest difference; our RMSE of all the available data is two to four times smaller. This implies our wind direction measurement has been more accurate and had better quality. This might be because the rather small sized and less powerful drone used by *Palomaki et al.* is more affected by the wind than our drone.

Overall the measurement quality seems to be comparable, with our wind speed measurement being a bit worse and wind direction measurement significantly better.

4.3.2 Comparison of results with [Wetz et al., 2021]

Wets et al. ended up choosing to use multiple small UAVs to estimate the wind. Their approach to the wind estimation was indirect, meaning instead of using an anemometer attached to a drone, they used logged IMU data to calculate the wind speed and direction.

Their measurement device was the quadrotor Holybro QAV250, a rather small drone, with motor to motor diameter of 0.25 meters and weight of only 0.65 kilograms.

In Table 4.14 the comparisons between bias and RMSEs of their and our results:

	Wind speed (m/s), *Wetz et al.*	Wind speed (m/s), our results	Difference (m/s)
Bias	0.004	0.336	-0.332
RMSE	0.23	0.745	-0.515
	Wind direction (°), *Wetz et al.*	Wind direction (°), our results	Difference (°)
Bias	9.5	-7.242	16.742
RMSE	7.5	13.3	-5.8

Table 4.14: Comparison of our results and results of *Wetz et al.*. The difference column shows the difference of values shown in the first two columns, in such way that $\Delta X = X_{Wetz} - X_{OR}$

Firstly, we can deduce that both our wind speed measurement bias and RMSE is higher than that of *Wetz et al.*. That would imply, that using the IMU data from multiple UAVs at the same time would be more accurate way of estimating wind speed. Of course our data has the bias caused by the propeller downwash present, and thus both the bias and RMSE should decrease once we have a way to filter out the effect of downwash properly.

Secondly, the absolute wind direction biases are of similar magnitude. The wind direction RMSEs are lower for the multiple small UAV method, but the difference is relatively smaller than the difference for the wind speed measurement.

Overall the method utilized by *Wetz et al.* has better quality and accuracy than the setup and method we used. Some changes that will be discussed in Section 5 should first be applied to our method, and then the comparison repeated to see how the measurements have improved.

4.3.3 Comparison of results with [Shimura et al., 2018]

In their research *Shimura et al.* used a direct approach for wind estimation. They used a middle sized UAV (SPIDER CS6, Luce Search Co., Ltd.) with horizontal dimensions of 95 centimeter x 95 centimeter and height of 40 cm. The weight of the drone was 3.8 kilograms.

The anemometer they used was a 2D ultrasonic anemometer (FT702, FT technologies), which was installed on a 47 centimeter high aluminium pole on top of the UAV. The wind data was logged on 1 Hz frequency. *Shimura et al.* had filtered out the effect of propeller downwash from the measurements.

In Table 4.15 the comparisons between bias and RMSEs of their and our results:

	Wind speed (m/s), *Shimura et al.*	Wind speed (m/s), our results	Difference (m/s)
Bias	0.1	0.336	-0.236
RMSE	0.6	0.745	-0.145
	Wind direction (°), *Shimura et al.*	Wind direction (°), our results	Difference (°)
Bias	-9.0	-7.242	-1.758
RMSE	12.0	13.3	-1.3

Table 4.15: Comparison of our results and results of *Shimura et al.*. The difference column shows the difference of values shown in the first two columns, in such way that $\Delta X = X_{Shimura} - X_{OR}$

Firstly, we can deduce that the wind speed bias is higher for our measurement setup. This is understandable, as the effect of propeller downwash has not been post-processed out of our wind speed data.

Secondly, the RMSEs of our and *Shimura et al.*'s measurements are very close to each other, with our RMSE value being slightly higher. This implies that the measurement setup utilized by *Shimura et al.* is of similar quality as our measurement arrangement. This is understandable, as the setup used by *Shimura et al.* is closest to the one used by us out of the three setups introduced in Sections 4.3.1, 4.3.2 and 4.3.3.

Thirdly, the wind direction biases are of similar magnitude and sign, with *Shimura et al.*'s setup having slightly higher bias.

Fourthly and lastly, the RMSEs of wind direction measurements are of similar magnitude, with a difference of less than 1.5°. This implies a similar quality of

measurement between our different measurement setups.

Overall the quality and accuracy of our measurement setup is comparable with that of *Shimura et al.*. This is a positive conclusion, as the setup used by *Shimura et al.* has also been used for atmospheric profiling up to 100 metres AGL. Having comparable measurement quality to a setup that has been used in atmospheric research reinforces the possibility of using a similar setup for operative meteorology. However, first some changes discussed in Section 5 should be considered and implemented, to see if this would yield even better quality of measurement.

5. Conclusions

In this thesis we discussed the possibility of using UAVs for wind measurements, as well as tried to find out the measurement quality of a dronebound anemometer by comparing its data with data from a traditional wind mast. Comparisons with previous studies were conducted as well as analysis on how wind data measured by dronebound anemometer fits the existing measurement standards. Lastly we tried to find out if the quality of our measurement arrangement is high enough for operational usage.

From our analysis we could make three main conclusions. Firstly, our measurement arrangement falls just a little short in measurement quality when compared with measurement arrangements used in previous studies.

Secondly, the data quality of our measurement arrangement is out of the WMO standards, as the typical magnitude of our wind speed error (0.745 m/s) is 0.245 m/s too high. Optimization to the measurement arrangement must be done, should sufficient measurement accuracy be obtained.

Thirdly and lastly, the measurement arrangement does not qualify for operational usage as is. Improvements to the measurement arrangement as well as data post-processing must be made before the setup can be used in operative wind measurements.

Overall the quality and accuracy of the measurement arrangement is surprisingly good for how simple the setup is. Close to comparable RMSEs to setups used in atmospheric research have been achieved with little optimisation and post-processing on Finnish Meteorological Institute's (FMI from now on) side. This speaks for the possibility of attaining top of the line UAV direct wind measurement setup, if some optimization is conducted.

For the possible optimization of the setup, a few things will be discussed below. These range from very simple additions to computationally and theoretically complex

post-processing.

Firstly, the anemometer could be attached to a gimball. This modification would make sure that the anemometer stays always perpendicular to the ground, no matter how much the UAV needs to tilt to stay stationary in the wind. This modification would reduce the effect of shadowing caused by the UAV tilting during measurement. This modification has been discussed by [Thielicke et al., 2021].

Secondly, a Real Time Clock -module (RTC-module from now on) should be installed into the data logger. At the moment the date and time needs to be set to the datalogger manually by using sudo commands. This can cause some slight, and completely unnecessary, temporal differences in the data. By including a RTC-module to the datalogger, we will get rid of this source of error completely, and at the same time will make the flight preparation easier and more straightforward by shaving of a step.

Thirdly, creation of correction functions should be discussed and considered. Comprehensive wind tunnel tests would need to be conducted for this optimization process to be possible, but the results should improve significantly. By conducting wind tunnel tests, the aerodynamical features of the measurement arrangement could be found. The effects of downwash could then be tested in different wind speeds and tilt angles. By using the aforementioned knowledge, empirical correction functions for the measurements could be created and applied, improving the measurement accuracy and quality. Creating these correction functions would require sufficiently good mathematical skills as well as plenty of time, but when ready, the results would be fruitful. Many previous studies such as [Shimura et al., 2018], [Hollenbeck et al., 2018], [Sekula et al., 2021] as well as [Wetz et al., 2021] have applied correction functions to their measurements. The usage of correction functions created for other measurement setups is not feasible, as aerodynamical properties differ between different types of UAVs.

Fourthly, installation of onboard compass, or comparable device, for more accurate orienting of the measuring device. At the moment the heading of the drone has to be approximated visually from the compass found in the app that is used while flying the drone. By adding another component that sends the drones heading to the pilot would easen the orienting of the drone. The component should also be located somewhere where the possible magnetic fields of the drone affected the direction of measurements as little as possible. Another possibility would be to use a software that allows the

wanted heading to be placed as an input. This would also require some hardware changes.

Fifthly and lastly, the application of the drones flight data to correct the measurements should be taken into consideration. In this study we have approximated the drone to be stationary during flight. This is of course not the case. The drone uses GPS to hold it's position, but the GPS signal is not completely accurate. The position of the drone can change up to 1.5 metres horizontally during hovering and vertically for some centimeters. GPS signal can also be lost in some cases. When GPS signal is lost, the drone tries to find the signal again by rotating in the air. By applying the drones flight data, we could first of all get rid of these erroneous data points and correct the wind speed measurement depending on the ground speed of the drone.

By considering the aforementioned optimization processes, it is realistic to presume that improved measurement quality as well as accuracy could be obtained. Applying these modifications is of course out of the scope of this thesis, and will be left for future consideration.

Acknowledgements

Especially I'd like to thank my supervisors Klaus, Jarkko and Jouni for the guidance while writing this thesis. Your help was irreplaceable and the work was made leagues easier by your insights and expertise.

I would also like to thank my superiors for giving me the chance to do my Master's thesis at FMI's Observation services unit, as well as all the colleagues whom I have had the privilege to work with in the last nine months.

Lastly I'd like to thank my parents and grandparents, who were suspiciously often asking me if the thesis was ever getting done, as well as my girlfriend bearing with me even though I got frustrated more than once while doing the data analysis.

Bibliography

[Barnston, 1992] Barnston, A. G. (1992). Correspondence among the correlation, rmse, and heidke forecast verification measures; refinement of the heidke score. *Weather and Forecasting*, 7(4):699 – 709.

[Britannica, 2023] Britannica, T. E. o. E. (2023). Atmospheric turbulence. *Encyclopedia Britannica*.

[Camuffo, 2019] Camuffo, D. (2019). Chapter 20 - measuring wind and indoor air motions. In Camuffo, D., editor, *Microclimate for Cultural Heritage (Third Edition)*, pages 483–511. Elsevier, third edition edition.

[Emeis and Turk, 2007] Emeis, S. and Turk, M. (2007). *Comparison of Logarithmic Wind Profiles and Power Law Wind Profiles and their Applicability for Offshore Wind Profiles*, pages 61–64.

[Galbis and Maestre, 2012] Galbis, A. and Maestre, M. (2012). *Vector Analysis Versus Vector Calculus*.

[Galton et al., 1885] Galton, F., Okamoto, S., and for National Eugenics, G. L. (1885). *Regression Towards Mediocrity in Hereditary Stature*. Harrison and Sons.

[Hollenbeck et al., 2018] Hollenbeck, D., Nunez, G., Christensen, L. E., and Chen, Y. (2018). Wind measurement and estimation with small unmanned aerial systems (suas) using on-board mini ultrasonic anemometers. In *2018 International Conference on Unmanned Aircraft Systems (ICUAS)*, pages 285–292.

[Holton, 2013] Holton, J. R. (2013). *An Introduction to Dynamic Meteorology, 5th Ed.*

[Kozera, 2018] Kozera, C. (2018). Military use of unmanned aerial vehicles – a historical study. *Safety & Defense*, 4:17–21.

[Neumann et al., 2012] Neumann, P. P., Asadi, S., Lilienthal, A. J., Bartholmai, M., and Schiller, J. H. (2012). Autonomous gas-sensitive microdrone: Wind vector estimation and gas distribution mapping. *IEEE Robotics & Automation Magazine*, 19(1):50–61.

[Palomaki et al., 2017] Palomaki, R. T., Rose, N. T., van den Bossche, M., Sherman, T. J., and Wekker, S. F. J. D. (2017). Wind estimation in the lower atmosphere using multirotor aircraft. *Journal of Atmospheric and Oceanic Technology*, 34(5):1183 – 1191.

[Pinto et al., 2021] Pinto, J. O., O'Sullivan, D., Taylor, S., Elston, J., Baker, C. B., Hotz, D., Marshall, C., Jacob, J., Barfuss, K., Piguet, B., Roberts, G., Omanovic, N., Fengler, M., Jensen, A. A., Steiner, M., and Houston, A. L. (2021). The status and future of small uncrewed aircraft systems (uas) in operational meteorology. *Bulletin of the American Meteorological Society*, 102(11):E2121 – E2136.

[Sekula et al., 2021] Sekula, P., Zimnoch, M., Bartyzel, J., Bokwa, A., Kud, M., and Necki, J. (2021). Ultra-light airborne measurement system for investigation of urban boundary layer dynamics. *Sensors*, 21(9).

[Shimura et al., 2018] Shimura, T., Inoue, M., Tsujimoto, H., Sasaki, K., and Iguchi, M. (2018). Estimation of wind vector profile using a hexarotor unmanned aerial vehicle and its application to meteorological observation up to 1000 m above surface. *Journal of Atmospheric and Oceanic Technology*, 35(8):1621 – 1631.

[Stull, 1988] Stull, R. B. (1988). *An Introduction to Boundary Layer Meteorol- ogy.*

[Thielicke et al., 2021] Thielicke, W., Hübert, W., Müller, U., Eggert, M., and Wilhelm, P. (2021). Towards accurate and practical drone-based wind measurements with an ultrasonic anemometer. *Atmospheric Measurement Techniques*, 14(2):1303–1318.

[Wetz et al., 2021] Wetz, T., Wildmann, N., and Beyrich, F. (2021). Distributed wind measurements with multiple quadrotor unmanned aerial vehicles in the atmospheric boundary layer. *Atmospheric Measurement Techniques*, 14(5):3795–3814.

[Wilson et al., 2022] Wilson, T. C., Brenner, J., Morrison, Z., Jacob, J. D., and Elbing, B. R. (2022). Wind speed statistics from a small uas and its sensitivity to sensor location. *Atmosphere*, 13(3).